Kinetics of a Gaussian random copolymer as a prototype for protein folding

E. G. Timoshenko,[*] Yu. A. Kuznetsov,[†] and K. A. Dawson

Theory Group, Centre for Soft Condensed Matter and Biomaterials, Department of Chemistry, University College Dublin,

Dublin 4, Ireland

(Received 9 February 1996; revised manuscript received 26 April 1996)

We develop the Gaussian self-consistent method for studying kinetics of random copolymers. For a fixed complexion of disorder the system is described by time- and disorder-dependent effective potentials. The self-consistent equations are then directly averaged over the quenched disorder, yielding a chain of differential equations with an enforced closure. This procedure allows us to avoid the use of the replica trick. Our method naturally incorporates the phase separation and glass order parameters and thus permits study of the complete phase diagram of the model. We believe that our approach may shed light on the kinetical aspects of the protein folding puzzle. [S1063-651X(96)09710-3]

PACS number(s): 87.15.By, 36.20.Ey

I. INTRODUCTION

One of the important challenges in the statistical-mechanical treatment of biopolymers is to understand the underlying mechanism of the highly unusual behavior of proteins [1,2]. It is well established that the one-dimensional sequence of amino acid residues, also called the primary structure, encodes the information about the unique three-dimensional conformation of a folded protein [3]. The native state in which a protein exhibits such properties is thermodynamically preferable under normal conditions within a living cell. The compactness of the globule in the native state is predominantly maintained by the hydrophobic effect [4] that forces the hydrophobic units to be mainly located inside the globule and the hydrophilic ones on the surface.

It has been recognized that the free-energy profile of proteins has an analogy with other disordered systems similar to spin glasses [5]. These frustrated systems have been much studied in the past decade [6,7]. As the relaxation times of glasses are typically very large, the system is trapped in a low-energy state separated from others by high-potential barriers. Similarly, the low-energy states of proteins correspond to minima of the free energy and the protein may be considered as "kinetically arrested" in one of its dominant conformations. This *freezing transition* occurs upon reducing the "effective temperature" of the polymer system. Finally, the protein reaches the unique global minimum of the free energy.

Another intriguing problem appears in considering the kinetics of protein folding. There are several different characteristic kinetic folding pathways for the globular proteins studied at present. For example, in Ref. [3] the authors consider proteins for which folding starts by a rapid collapse from a random coil state to a semicompact molten globule and then proceeds by a slow search to a state from which the chain will eventually access the native state. The number of available conformations of a polypeptide chain grows exponentially with the chain length and is therefore extremely large. Nevertheless, it is known experimentally that proteins do fold into a unique native state in just a matter of seconds. The Levinthal paradox is that the chain is somehow able to find its native configuration without extensively exploring all possible conformations.

The mechanism responsible for this restriction of accessible conformations during folding is probably also related to the kinetics of spin-glass-like systems [3]. However, in theory this connection has not as yet been really explained. Several approaches have been proposed to explain the Levinthal paradox dealing with folding kinetics along the so-called "preferred pathways" on the free-energy landscape [8–12]. These approaches share some common features in that they explain the tendency of folding towards the native conformation, but they differ in many details. Although much understanding has been achieved in the above-quoted models, there is still uncertainty remaining in the detailed laws for realistic protein sizes. The final resolution of the protein folding puzzle and elucidation of the kinetic laws that govern this process would shed some light on the questions related to the origin of life in the prebiotic and early biotic environments and might have implications for the theory of evolution. Practical consequences could also emerge for protein engineering.

The statistical-mechanical approach [13] to protein folding is based on the investigation of the properties of simple models of heteropolymers. The simplest approximation for a protein is a random heteropolymer. In the *sequence model* [14] monomer types are represented by random variables $\{\Lambda_m\}$, with a given distribution of disorder (e.g., binary or Gaussian), that determine the excluded-volume interactions between pairs of amino acids.

There have been extensive studies of the equilibrium properties of the model carried out using the replica trick of the spin-glass theory [14–18]. The success of these studies was significant in two respects. First, it has been established that even a simple Gaussian random copolymer undergoes the freezing transition and thus this property is probably typical for all random heteropolymers. Second, an understanding of the role of microphase separation [19] and its competition with freezing has been achieved. It was shown in Refs.

————————
[*]Electronic address: timosh@fiachra.ucd.ie

[†]Also at the Institute of Theoretical and Experimental Biophysics, Russian Academy of Sciences, Pushchino, 142292, Russia.

[14,16] that for a stiff chain freezing prevents microphase separation. If the chain is flexible enough the freezing occurs at a lower temperature with a background of phase separation.

As a limitation of these works we note that they were based only upon a special form of the interaction matrix, corresponding to the so-called symmetric ''charged'' model. Another disadvantage of these approaches lies in their validity only for a globular state, where it is possible to use the ground-state dominance and constant density approximations. We would like to emphasize that to really understand the protein folding problem of kinetics one needs a method that is equally reliable for both the extended coil and compact globular states.

It has become clear that to ensure kinetic reliability of folding sequences should be more special than simply random. This is important in order to make the native conformation stable even in a model with noisy distorted potentials [20]. The interactions of a kinetically foldable protein should obey the ''minimal frustration principle'' [8] requiring minimization of frustration or, in other words, the ratio of glass to folding temperatures. One of the possibilities to satisfy this principle is to consider ''selected'' [21], ''designed'' [22], or ''imprinted'' [23] sequences. The principles of the energy landscape analysis have been studied and confirmed in many simulations of simple models [9–11]. It was found that for fast folding sequences there should be a special interplay between the energy frustration and entropic barriers.

These suggestions are certainly interesting and perhaps quite important for explaining the role of evolutionary selection within the ''primordial soup.'' However, they deal with the next level of complexity in models of proteins. Our belief is that, first of all, it would be interesting to construct an analytic theory of kinetics of protein folding for a random sequence model and study the kinetic laws there. Later on the knowledge about the sequences distribution discovered in other approaches may be used in such a theory, thereby making it more realistic for proteins.

It is well established that the frozen phase exists for random copolymers. Thus the spin-glass mechanisms restricting the available conformations of the chain do help it search (whether kinetically or quasistatically) for a state with quite few conformations left. Whether an arbitrary random sequence would be able to fold from this prior state, which probably might be interpreted as the molten globule, to the true native state, i.e., undergo *renaturation*, remains an open question. In this paper we find evidence for the affirmative answer of this question. We also discover that this transition is accompanied by a decrease of the globule size and a profound restructuring of the microdomain structure exhibited in the phase-separation order parameter. In other words, renaturation may be considered as a rather complex transition described by the glassy order parameter and manifested in the change of many observable characteristics of the globule.

Our method is essentially designed to make feasible the study the kinetics of protein folding at a later point. There are numerous analytical works on the equilibrium aspects of the problem [14–18]. However, the knowledge about kinetics of the process is restricted to Monte Carlo simulations on a lattice [9,10,24–26]. Evidently one would hope to be able

to compliment these Monte Carlo simulations by an analytical theory as well.

In this work we study the kinetics of a random sequence model using the Gaussian self-consistent approach. This approach [27,28], which resembles the time-dependent Hartree approximation and reduces to the variational Gibbs-Bogoliubov variational estimate at equilibrium, has the merit of being precisely defined, flexible, and of general applicability to many classes of problems. A strong argument in favor of our method is the good agreement with Monte Carlo simulation for the homopolymer kinetics performed on a lattice [29].

Our approach leads to a set of nonlinear and highly coupled differential equations for the main observables of the system. Although their detailed analytical study is a rather complicated technical task, it is relatively simple to solve these equations numerically. The qualitative behavior of the solution that we find appears very encouraging.

In this paper we will present our thinking about the problem in the language of statistical mechanics. These ideas are further discussed and explained using more physically appealing language elsewhere [31].

II. METHOD

To avoid confusion in this paper we shall denote the monomer spatial positions by capital characters $\mathbf{X}_m$ and their Fourier transforms by the lowercase ones $\mathbf{x}_q$, and similarly for other distributions along the chain. The Fourier transformations for ring polymer are defined as

$$\mathbf{X}_m = \sum_{q=0}^{N-1} f_m^{(-q)} \mathbf{x}_q, \quad \mathbf{x}_q = \frac{1}{N} \sum_{m=0}^{N-1} f_m^{(q)} \mathbf{X}_m, \quad (1)$$

$$f_m^{(q)} \equiv \exp\left(\frac{2\pi i q m}{N}\right), \quad (2)$$

where N is the degree of polymerization. In the absence of hydrodynamic effect [32] the exact Langevin equation for the sequence model of a random copolymer may be written in terms of the Fourier modes as [33],

$$\zeta \frac{d}{dt} \mathbf{x}_q(t) = -\frac{\partial H}{\partial \mathbf{x}_{-q}} + \boldsymbol{\eta}_q(t), \quad (3)$$

$$\langle \eta_q^\alpha(t) \eta_{q'}^{\alpha'}(t') \rangle = 2k_B T \zeta \delta_{q+q',0} \delta^{\alpha\alpha'} \delta(t-t'), \quad (4)$$

where $\zeta = N\zeta_b$ and ζ_b is the bare friction constant. The interaction potential $H = \bar{H} + \tilde{H}$ consists of the homopolymeric $\bar{H}$ and the disordered $\tilde{H}$ parts, respectively,

$$\bar{H} = \frac{\kappa}{2} \sum_n (\mathbf{X}_{n+1} - \mathbf{X}_n)^2 + \sum_{L>2} \bar{u}_L \sum_{\{m\}} \prod_{i=1}^{L-1} \delta(\mathbf{X}_{m_i} - \mathbf{X}_{m_{i+1}}), \quad (5)$$

$$\tilde{H} = \frac{1}{2} \sum_{m_1, m_2} (\Lambda_{m_1} + \Lambda_{m_2}) \delta(\mathbf{X}_{m_1} - \mathbf{X}_{m_2}), \quad (6)$$

where κ is the spring constant, $\bar{u}_L$ are the virial coefficients of the excluded-volume interactions, and the summation over

$\{m\}$ includes all values of indices $m_1, \ldots, m_L$ with $m_i \neq m_{i+1}$. Here Λ_m are independent random variables [34] with the Gaussian distribution of disorder

$$P(\{\Lambda\}) = \prod_m \frac{1}{(2\pi\Delta^2)^{1/2}} \exp\left(-\frac{\Lambda_m^2}{2\Delta^2}\right). \qquad (7)$$

The Fourier transforms $\{\lambda\}$ are also independent random Gaussian variables with zero mean value and dispersion $\overline{\Delta}^2$,

$$\overline{\lambda_q \lambda_{q'}} = \overline{\Delta}^2 \delta_{q+q',0}, \quad \overline{\Delta}^2 \equiv \Delta^2/N. \qquad (8)$$

Henceforth we use the brackets $\langle A \rangle$ to denote the statistical averages over the noise and initial ensemble of monomer positions $\{\mathbf{X}(t=0)\}$ and the bar $\overline{A}$ to denote averages over the quenched distribution of disorder $\{\Lambda\}$.

We start by noting that for a given complexion of disorder Eq. (3) is exactly identical to the Langevin equations for arbitrary heteropolymer, with the two-body virial coefficients that are given by the formula

$$u_{m_1 m_2}^{(2)} = \overline{u}_2 + \frac{1}{2}(\Lambda_{m_1} + \Lambda_{m_2}). \qquad (9)$$

In our earlier work [35] we have shown that such a system could be successfully studied in the framework of the Gaussian self-consistent method with a nondiagonal self-consistent potential. Since there are no *a priori* symmetry properties along the chain, when we use the Fourier variables (1) the self-consistent potential is nondiagonal and denoted by $V_{qp}(t)$. Thus we replace the exact Langevin equation (3) by a linear stochastic ensemble

$$\zeta \frac{d}{dt} \mathbf{x}_q = -\sum_p V_{qp}(\{\lambda\},t)\mathbf{x}_p + \boldsymbol{\eta}_q(t), \qquad (10)$$

where the potential V_{qp} is to be determined self-consistently from the exact equations. The potential has a homopolymeric diagonal part and a nondiagonal part describing the disorder that, according to Eq. (6), should be taken as an arbitrary linear combination of the disorder variables

$$V_{qp}(\{\lambda\},t) \equiv V_q(t)\delta_{qp} + \sum_r U_{qpr}(t)\lambda_r. \qquad (11)$$

Finally, having derived as many self-consistent equations as there are unknown functions, one has to average over the quenched disorder. This can be accomplished for the Gaussian disorder perturbatively by application of the Wick theorem

$$\overline{A(\{\Lambda\})} = \exp\left(\frac{\Delta^2}{2}\sum_n \frac{\partial^2}{\partial \Lambda_n^2}\right)\Bigg|_{\{\Lambda\}=0} A(\{\Lambda\}). \qquad (12)$$

Evidently, such a program, although feasible, would be rather difficult to realize in practice. On one hand, the potential with three indices would give rise to very cumbersome expressions, making analysis complicated. On the other hand, there is a serious problem in that the self-consistency equations are not closed, but constitute an infinite chain of

Bogoliubov-like equations. This, of course, could be avoided at the level of the Gaussian theory, but at the price of dealing with extremely complicated integro-differential equations instead of simple differential ones. Indeed, the higher-order correlation functions may be explicitly calculated order by order in $\{\Lambda\}$ applying the formal integration of the linear ensemble (10). Naturally, both approaches lead to equivalent results, although the proof is not straightforward for the general case. The most satisfactory procedure is to construct the Bogoliubov chain and close it at some order, either by a nonperturbative ansatz or just in a given order of the dispersion Δ^2 of the self-consistent perturbative scheme. Although similar methods have proved to be effective in statistical mechanics, for random copolymers, due to the connectivity and higher-order virial terms, one finds a rather complicated set of equations. In the present paper we pursue the least ambitious route; that is, we shall study the effects of randomness in lowest order (Δ^2) and leave more complicated higher-order calculations for future consideration. Since we apply a self-consistent treatment and deal with ''fully dressed'' quantities we may expect to be able to probe relatively large dispersions of disorder.

At first order several fortunate simplifications appear that make our analysis much easier. In fact, one will see later that some of the observations that follow trivially in this order persist in higher orders as well. We shall emphasize such points and also indicate the physical reasons for them in the Conclusion.

First, let us discuss the equal-time correlation functions $\langle \mathbf{x}_q(t)\mathbf{x}_p(t) \rangle$. These must be considered to be nondiagonal for a given complexion of disorder. However, after averaging over $\{\lambda\}$ they become diagonal (see the Appendix for more detail), reflecting the translational invariance along the chain after integrating out the disorder. Thus we introduce one of the observables of interest

$$\mathcal{F}_q(t) \equiv \overline{F_q(t)}, \quad F_q(t) = \frac{1}{3}\langle |\mathbf{x}_q|^2(t)\rangle. \qquad (13)$$

Integration of the linear equation (10) yields a result that may be presented in matrix notation

$$\mathbf{x}(t) = \Gamma(\{\lambda\};t,0)\cdot\mathbf{x}(0) + \frac{1}{\zeta}\int_0^t dt'\Gamma(\{\lambda\};t,t')\cdot\boldsymbol{\eta}(t'), \qquad (14)$$

$$\Gamma(\{\lambda\};t,t') \equiv T\text{-}\exp\left(-\frac{1}{\zeta}\int_{t'}^t d\tau\, V(\{\lambda\},\tau)\right). \qquad (15)$$

Thus, since $\mathbf{x}_q(t)$ is linear in the initial condition $\mathbf{x}_q(0)$ and the noise, the correlation functions $F_q(t)$ can be expressed via the kernels $\Gamma(\{\lambda\};t,t')$. Similarly, multiplying Eq. (3) by $\mathbf{x}_{-q}(t)$ and performing evaluations analogous to those of Refs. [27,28], one can derive

$$\frac{\zeta}{2}\frac{d}{dt}F_q(t) = k_B T - \frac{1}{3}\left\langle \mathbf{x}_{-q}\frac{\partial H}{\partial \mathbf{x}_{-q}}\right\rangle, \qquad (16)$$

where the latter average may be recovered by a differentiation of the mean energy with respect to a set of parameters $\{\gamma\}$:

$$\left\langle \mathbf{x}_{-q} \frac{\partial H}{\partial \mathbf{x}_{-q}} \right\rangle = \frac{\partial \langle H \rangle}{\partial \gamma_{-q}} \bigg|_1 . \tag{17}$$

By averaging the energy per sample we obtain

$$\langle H \rangle = \frac{3\kappa}{2} \sum_m D_{m,m-1} + \frac{1}{2(2\pi)^{3/2}} \sum_{m,m'} (\Lambda_m + \Lambda_{m'}) D_{mm'}^{-3/2}$$

$$+ \frac{\bar{u}_2}{(2\pi)^{3/2}} \sum_{m,m'} D_{mm'}^{-3/2} + \frac{\bar{u}_3}{(2\pi)^3}$$

$$\times \sum_{m,m',m''} (D_{mm'} D_{m''m'} - D_{mm'm''}^2)^{-3/2}$$

$$+ (\text{four-body terms}) + \cdots . \tag{18}$$

Here we have used the notation

$$D_{mm'} = \frac{1}{3} \sum_{q,p} \gamma_q \gamma_p c_{mm'}^{(q)} c_{mm'}^{(p)} \langle \mathbf{x}_q \mathbf{x}_p \rangle , \tag{19}$$

$$c_{mm'}^{(q)} \equiv f_m^{(-q)} - f_{m'}^{(-q)} , \tag{20}$$

where we have introduced the auxiliary parameters γ_q, which are set equal to unity at the end of our calculations. Then the quantities (19) acquire a transparent meaning

$$D_{mm'}(\gamma_q = 1) \equiv \frac{1}{3} \langle (\mathbf{X}_m - \mathbf{X}_{m'})^2 \rangle = \sum_q d_{mm'}^{(q)} F_q , \tag{21}$$

$$d_{mm'}^{(q)} = 2 \left(1 - \cos \frac{2\pi q (m - m')}{N} \right) . \tag{22}$$

Finally, the three-body correlations $D_{mm'm''}$ are defined according to

$$D_{mm'm''} = \frac{1}{3} \sum_{q,p} \gamma_q \gamma_p c_{mm'}^{(q)} c_{m''m}^{(p)} \langle \mathbf{x}_q \mathbf{x}_p \rangle \tag{23}$$

and the higher-order terms may be found in Ref. [36]. Note that for $\gamma_q = 1$ there are simple reduction relations

$$D_{mm'm''}(\gamma_q = 1) \equiv \frac{1}{3} \langle (\mathbf{X}_m - \mathbf{X}_{m'})(\mathbf{X}_{m''} - \mathbf{X}_{m'}) \rangle$$

$$= \sum_q d_{mm'm''}^{(q)} F_q , \tag{24}$$

$$d_{mm'm''}^{(q)} = \frac{1}{2} (d_{mm'}^{(q)} + d_{m''m'}^{(q)} - d_{mm''}^{(q)}) . \tag{25}$$

III. WEAK FLUCTUATIONS OF DISORDER

A. Derivation of the kinetic equations

In this section we shall calculate the quenched disorder average of Eq. (18) to order Δ^2. Using the Wick theorem (12) and keeping only the lowest order it is possible to derive the relations

$$\overline{\langle H \rangle} = E_0 + E_1 + E_2 , \tag{26}$$

$$E_0 = \frac{3\kappa}{2} \sum_m \mathcal{D}_{m,m-1} + \hat{u}_2 \sum_{m,m'} \mathcal{D}_{mm'}^{-3/2}$$

$$+ \hat{u}_3 \sum_{m,m',m''} (\mathcal{D}_{mm'} \mathcal{D}_{m''m'} - \mathcal{D}_{mm'm''}^2)^{-3/2} + (\text{four-body terms}) + \cdots , \tag{27}$$

$$E_1 = -\Delta^2 \hat{1} \frac{3}{2} \sum_{m,m'} \frac{\mathcal{D}_{mm';m}}{\mathcal{D}_{mm'}^{5/2}} , \tag{28}$$

$$E_2 = \Delta^2 \hat{u}_2 \frac{15}{8} \sum_{m,m',r} \frac{(\mathcal{D}_{mm';r})^2}{\mathcal{D}_{mm'}^{7/2}} + \Delta^2 \hat{u}_3 \frac{15}{8} \sum_{m,m',m'',r} \frac{(\mathcal{D}_{mm'} \mathcal{D}_{m''m';r} + \mathcal{D}_{m''m'} \mathcal{D}_{mm';r} - 2 \mathcal{D}_{mm'm''} \mathcal{D}_{mm'm'';r})^2}{(\mathcal{D}_{mm'} \mathcal{D}_{m''m'} - \mathcal{D}_{mm'm''}^2)^{7/2}}$$

$$- \Delta^2 \hat{u}_3 \frac{3}{2} \sum_{m,m',m'',r} \frac{(\mathcal{D}_{mm';r} \mathcal{D}_{m''m';r} - (\mathcal{D}_{mm'm'';r})^2)}{(\mathcal{D}_{mm'} \mathcal{D}_{m''m'} - \mathcal{D}_{mm'm''}^2)^{5/2}} + \cdots . \tag{29}$$

Here the term E_0 represents the homopolymerlike contribution, E_1 is the main interaction part, and E_2 describes the dispersion along the chain. We have also introduced the rescaled virial coefficients $\hat{u}_L = (2\pi)^{-3(L-1)/2} \bar{u}_L$ and $\hat{1} \equiv (2\pi)^{-3/2}$.

In the derivation above we have utilized the Taylor expansion

$$D_{mm'} = D_{mm'}(0) + \sum_r \Lambda_r D_{mm';r}(0)$$

$$+ \frac{1}{2} \sum_{r,r'} \Lambda_r \Lambda_{r'} D_{mm';rr'}(0) + \cdots . \tag{30}$$

The Taylor coefficients are simply related to the averages

$$\mathcal{D}_{mm'} \equiv \overline{D_{mm'}} = D_{mm'}(0) + \frac{\Delta^2}{2} \sum_r D_{mm';rr}(0), \quad (31)$$

$$\mathcal{D}_{mm';r} \equiv \Delta^{-2} \overline{\Lambda_r D_{mm''}} = D_{mm';r}(0). \quad (32)$$

We can also express the terms of E_2 as cumulants,

$$\Delta^2 \sum_r \mathcal{D}_{mm';r} \mathcal{D}_{m''m';r} = \overline{D_{mm'} D_{m''m'}}^{(c)} \equiv \overline{D_{mm'} D_{m''m'}}$$

$$- \overline{D_{mm'}} \, \overline{D_{m''m'}}, \quad (33)$$

and so forth.

It is important to stress that after the integration over the disorder, averages of the Fourier modes become diagonal,

$$\frac{1}{3} \overline{\langle \mathbf{x}_{-q} \mathbf{x}_p \rangle} = \delta_{qp} \mathcal{F}_q. \quad (34)$$

This implies that $\mathcal{D}_{mm'} = \mathcal{D}_k$, where $k = m - m'$, and hence the translational invariance along the chain is restored. In view of this we may rewrite the interaction term E_1 in another form

$$E_1 = -\frac{3N}{2(2\pi)^{3/2}} \sum_k \frac{\Phi_k}{\mathcal{D}_k^{5/2}}, \quad (35)$$

$$\Phi_k = \frac{1}{N} \overline{\sum_m \Lambda_m D_{mm+k}} = \sum_{q,p} d_k^{(q,p)} \varphi_{qp}, \quad (36)$$

where the new variable is defined by

$$\varphi_{qp}(t) \equiv \overline{\phi_{qp}(t)}, \quad \phi_{qp}(t) = \frac{1}{3} \lambda_{q-p} \langle \mathbf{x}_{-q}(t) \mathbf{x}_p(t) \rangle \quad (37)$$

and the coefficients

$$d_k^{(q,p)} = \frac{1}{2} (d_k^{(q)} + d_k^{(p)} - d_k^{(q-p)}) \quad (38)$$

and $d_{k_1 k_2}^{(q,p)}$ are similarly expressed via $d_k^{(q,p)}$ by (25).

In the variational principle one should add to the trial Hamiltonian the structures that appear in the interaction (6). Thus we take the trial Hamiltonian H_0 as a combination of two observables (13) and (37),

$$H_0 = \frac{1}{2} \sum_q V_q \mathbf{x}_{-q} \mathbf{x}_q + \frac{1}{2} \sum_{q,p} U_{qp} \lambda_{q-p} \mathbf{x}_{-q} \mathbf{x}_p. \quad (39)$$

Note that in the coordinate space the Hamiltonian may be written in the form

$$H_0 = \frac{1}{2} \sum_{m,m'} \left(\mathcal{V}_{m-m'} + \sum_n \mathcal{U}_{m-n,m'-n} \Lambda_n \right) (\mathbf{X}_m - \mathbf{X}_{m'})^2, \quad (40)$$

where $\mathcal{V}$ and $\mathcal{U}$ are obtained by Fourier transformation from V and U. This structure corresponds to a restricted form of the interaction matrix (11),

$$U_{qpr}(t) = U_{qp}(t) \delta_{r,q-p}. \quad (41)$$

In the Appendix we prove that such a form of the effective potential ensures the diagonality property (34) at arbitrary order of the disorder dispersion.

From the trial Hamiltonian (37) we immediately get the equation of motion

$$\frac{\zeta}{2} \frac{d}{dt} F_q(t) = k_B T - V_q F_q - \sum_p U_{qp} \phi_{qp}. \quad (42)$$

This can be directly averaged over the disorder. As for the equation for $\varphi_{qp}(t)$, it is, strictly speaking, not closed due to the second term in the trial Hamiltonian. Meanwhile, ignoring higher-order terms in $\overline{\Delta}^2$, it is straightforward to write down a system of two closed equations of motion

$$\frac{\zeta}{2} \frac{d}{dt} \mathcal{F}_q(t) = k_B T - V_q \mathcal{F}_q - \sum_p U_{qp} \varphi_{qp}, \quad (43)$$

$$\zeta \frac{d}{dt} \varphi_{qp}(t) = -(V_q + V_p) \varphi_{qp} - \overline{\Delta}^2 U_{qp}(\mathcal{F}_q + \mathcal{F}_p). \quad (44)$$

Note also that the different-time correlation functions

$$\mathcal{G}_q(t,t') = \frac{1}{3} \overline{\langle \mathbf{x}_{-q}(t') \mathbf{x}_q(t) \rangle}, \quad (45)$$

$$\chi_{qp}(t,t') = \frac{1}{3} \overline{\lambda_{q-p} \langle \mathbf{x}_{-q}(t') \mathbf{x}_p(t) \rangle} \quad (46)$$

satisfy similar equations for $t' < t$,

$$\zeta \frac{d}{dt} \mathcal{G}_q(t,t') = -V_q(t) \mathcal{G}_q(t,t') - \sum_p U_{qp}(t) \chi_{qp}(t,t'), \quad (47)$$

$$\zeta \frac{d}{dt} \chi_{qp}(t,t') = -V_p(t) \chi_{qp}(t,t') - \overline{\Delta}^2 U_{qp}(t) \mathcal{G}_q(t,t'). \quad (48)$$

The initial conditions are simply $\mathcal{G}_q(t',t') = \mathcal{F}_q(t')$ and $\chi_{qp}(t',t') = \varphi_{qp}(t')$. Therefore, integration of the second equation gives

$$\chi_{qp}(t',t) = \varphi_{qp}(t') G_p(t,t') - \frac{\overline{\Delta}^2}{\zeta}$$

$$\times \int_{t'}^t d\tau \sum_p G_p(t,t') G_p^{-1}(\tau,t') U_{qp}(\tau) \mathcal{G}_q(\tau,t'),$$

$$G_p(\tau,t') = \exp\left(-\frac{1}{\zeta} \int_{t'}^\tau dt'' V_p(t'') \right). \quad (49)$$

Then Eq. (47) may be rewritten as a non-Markovian equation

$$\zeta \frac{d}{dt} \mathcal{G}_q(t,t') = -V_q(t) \mathcal{G}_q(t,t') + \int_{t'}^t d\tau \Xi_q(t,\tau;t') \mathcal{G}_q(\tau,t')$$

$$- \sum_p U_{qp}(t) G_p(t,t') \varphi_{qp}(t'), \quad (50)$$

$$\Xi_q(t,\tau;t') \equiv \frac{\overline{\Delta}^2}{\zeta} \sum_p G_p(t,t') G_p^{-1}(\tau,t') U_{qp}(t) U_{qp}(\tau),$$
(51)

with a memory kernel given by $\Xi_q(t,\tau;t')$.

Now let us consider the cumulant terms in Eq. (29). Since they are of higher than quadratic order we should not add them to the trial Hamiltonian at the level of the Gaussian theory. This permits us to use the restriction $(1/3)\langle \mathbf{x}_{-q}\mathbf{x}_p \rangle \lambda_r = \delta_{r,q-p}\varphi_{qp}$ in the calculation. Performing the Fourier transformation and some simple algebra, we can prove that the cumulants (33) depend only on the differences of their indices $k_1 = m - m'$ and $k_2 = m'' - m'$,

$$\overline{D_{mm'}D_{m''m'}}^{(c)} = \overline{D_{k_1}D_{k_2}}^{(c)}, \quad D_k \equiv D_{0\,k}.$$
(52)

Moreover, they may be related to the order parameters (37)

$$\overline{D_{k_1}D_{k_2}}^{(c)} = \overline{\Delta}^{-2} \sum_{q,q',p} d_{k_1}^{(q,q')} d_{k_2}^{(p,p+q-q')} \varphi_{qq'}\varphi_{pp+q-q'}.$$
(53)

Therefore, these variables describe sample to sample fluctuations and are typical glass order parameters [7].

There are other similar order parameters that can be calculated. For example, it is instructive to study the cumulants of the Fourier modes $\overline{F_q F_p}^{(c)}$. Using the equation of motion (42), we obtain the differential equation

$$\frac{\zeta}{2}\frac{d}{dt}\overline{F_q F_p}^{(c)} = -(V_q + V_p)\overline{F_q F_p}^{(c)}$$
$$- (U_{qq}\varphi_{qq}\mathcal{F}_p + U_{pp}\varphi_{pp}\mathcal{F}_q).$$
(54)

The latter can be immediately integrated and expressed through φ_{qq}. In fact, due to the equation of motion (44) and the zero initial condition there is a remarkable relation

$$\overline{F_q(t)F_p(t)}^{(c)} = \overline{\Delta}^{-2}\varphi_{qq}(t)\varphi_{pp}(t).$$
(55)

This result may be easily generalized in a similar fashion,

$$\frac{1}{9}\overline{\langle \mathbf{x}_q\mathbf{x}_{q'}\rangle\langle \mathbf{x}_p\mathbf{x}_{p'}\rangle}^{(c)} = \overline{\Delta}^{-2}\varphi_{-pp'}\varphi_{-qq'}\delta_{q+q'+p+p',0}.$$
(56)

If we recall that the squared radius of gyration is just the sum

$$R_g^2 = \sum_{q\neq 0} F_q,$$
(57)

from (55) one derives the sample to sample fluctuation of the squared radius of gyration

$$\overline{R_g^2 R_g^2}^{(c)} = \overline{\Delta}^{-2}\Upsilon^2,$$
(58)

where

$$\Upsilon \equiv \overline{\lambda_0 R_g^2} = \sum_{q\neq 0} \varphi_{qq}.$$
(59)

Note that the cumulants $\overline{F_q F_p}^{(c)}$ are only connected to the fluctuations of the composition λ_0,

$$\varphi_{qq} = \overline{\lambda_0 F_q}.$$
(60)

The cumulants of the spatial correlations (53) [and the quantities (56)] are more nontrivial because they contain contributions nondiagonal in the Fourier indices. Once again, the quantity Υ is a typical "glass" order parameter. By definition it is equal to the fluctuation of the squared radius of gyration over different sequences. Such a fluctuation is big inside the "glassy" phase due to strong correlations of different copies of the system in the standard replica trick language [6,7].

Another order parameter of interest

$$\Psi = \frac{1}{6N^2}\sum_{mm'} \overline{(\Lambda_m + \Lambda_{m'} - 2\lambda_0)D_{mm'}},$$
(61)

$$\Psi = \sum_{q\neq p;q,p\neq 0} \varphi_{qp}$$
(62)

is actually related to the phase separation. Thus let us consider the limit of only two types of monomers: hydrophobic A, with $\lambda_A = -1$, and hydrophilic B, with $\lambda_B = 1$. Suppose that there are N_A monomers of type A and N_B of type B, so that the composition $\lambda_0 = (1/N)\Sigma_m\Lambda_m$ may be expressed through the concentrations $n_A \equiv N_A/N$ and $n_B \equiv N_B/N$, with $n_A + n_B = 1$, simply as $\lambda_0 = n_B - n_A$. Then it is easy to show that Ψ is reduced to the quantity

$$\Psi = 4n_A n_B\{n_B[R_g^2(B) - R_g^2(A,B)] - n_A[R_g^2(A) - R_g^2(A,B)]\},$$
(63)

where we have introduced the partial radii of gyration

$$R_g^2(A) = \frac{1}{2N_A^2}\sum_{m,m'\in A} D_{mm'}, \quad R_g^2(B) = \frac{1}{2N_B^2}\sum_{m,m'\in B} D_{mm'},$$
(64)

$$R_g^2(A,B) = \frac{1}{N_A N_B}\sum_{m\in A,m'\in B} D_{mm'}.$$
(65)

For equal concentrations $n_A = n_B = 1/2$ this reduces just to $\Psi = [R_g^2(B) - R_g^2(A)]/2$.

B. Effective potentials

Now having introduced the basic observables and derived the equations of motion, we only have to self-consistently determine the effective potentials. These are to be found from the equation

$$\left\langle \mathbf{x}_{-q}\frac{\partial H}{\partial \mathbf{x}_{-q}}\right\rangle_0 = \left\langle \mathbf{x}_{-q}\frac{\partial H_0}{\partial \mathbf{x}_{-q}}\right\rangle_0,$$
(66)

where $\langle \ \rangle_0$ designates the average over the trial distribution.

A somewhat lengthy calculation using Eqs. (17) and (26)–(29) finally leads us to the closure relations [37]

$$\frac{V_q}{N} = \kappa d_1^{(q)} - \hat{u}_2 \sum_k \frac{d_k^{(q)}}{\mathcal{D}_k^{5/2}} - \hat{u}_3 \sum_{k_1,k_2} \frac{Y_1(q;k_1,k_2)}{Y_0(k_1,k_2)^{5/2}}$$
$$+ \frac{5}{2}\hat{1}\sum_k \frac{d_k^{(q)}\Phi_k}{\mathcal{D}_k^{7/2}} - \hat{u}_2 \frac{35}{8}\sum_k \frac{d_k^{(q)}P_{k,k}}{\mathcal{D}_k^{9/2}}$$
$$- \hat{u}_3 \frac{35}{8}\sum_{k_1,k_2} \frac{Y_2(k_1,k_2)Y_1(q;k_1,k_2)}{Y_0(k_1,k_2)^{9/2}}$$
$$+ \hat{u}_3 \frac{5}{2}\sum_{k_1,k_2} \frac{Y_3(k_1,k_2)Y_1(q;k_1,k_2)+Y_6(q;k_1,k_2)}{Y_0(k_1,k_2)^{7/2}}, \tag{67}$$

and for the nondiagonal effective potential

$$\frac{U_{qp}}{N} = -\hat{1}\sum_k \frac{d_k^{(q,p)}}{\mathcal{D}_k^{5/2}} + \hat{u}_2 \frac{5}{2}\sum_k \frac{d_k^{(q,p)}\overline{\Delta}^{-2}P_k^{(q-p)}}{\mathcal{D}_k^{7/2}}$$
$$+ \hat{u}_3 \frac{5}{2}\sum_{k_1,k_2} \frac{Y_4(q,p;k_1,k_2)}{Y_0(k_1,k_2)^{7/2}} - \hat{u}_3 \sum_{k_1,k_2} \frac{Y_5(q,p;k_1,k_2)}{Y_0(k_1,k_2)^{5/2}}. \tag{68}$$

Here we have used the set of definitions

$$Y_0(k_1,k_2) = \mathcal{D}_{k_1}\mathcal{D}_{k_2} - \mathcal{D}_{k_1 k_2}^2, \tag{69}$$

$$Y_1(q;k_1,k_2) = d_{k_1}^{(q)}\mathcal{D}_{k_2} + d_{k_2}^{(q)}\mathcal{D}_{k_1} - 2d_{k_1 k_2}^{(q)}\mathcal{D}_{k_1 k_2}, \tag{70}$$

$$Y_2(k_1,k_2) = \mathcal{D}_{k_1}^2 P_{k_2,k_2} + \mathcal{D}_{k_2}^2 P_{k_1,k_1} + 4\mathcal{D}_{k_1 k_2}^2 P_{k_1 k_2,k_1 k_2}$$
$$+ 2\mathcal{D}_{k_1}\mathcal{D}_{k_2}P_{k_1,k_2} - 4\mathcal{D}_{k_1 k_2}(\mathcal{D}_{k_2}P_{k_1,k_1 k_2}$$
$$+ \mathcal{D}_{k_1}P_{k_2,k_1 k_2}), \tag{71}$$

$$Y_3(k_1,k_2) = P_{k_1,k_2} - P_{k_1 k_2,k_1 k_2}, \tag{72}$$

$$Y_4(q,p;k_1,k_2) = \overline{\Delta}^{-2}[\mathcal{D}_{k_1}^2 d_{k_2}^{(q,p)}P_{k_2}^{(q-p)} + \mathcal{D}_{k_2}^2 d_{k_1}^{(q,p)}P_{k_1}^{(q-p)}$$
$$+ 4\mathcal{D}_{k_1 k_2}^2 d_{k_1 k_2}^{(q,p)}P_{k_1 k_2}^{(q-p)}$$
$$+ \mathcal{D}_{k_1}\mathcal{D}_{k_2}(d_{k_1}^{(q,p)}P_{k_2}^{(q-p)} + d_{k_2}^{(q,p)}P_{k_1}^{(q-p)})$$
$$- 2\mathcal{D}_{k_1 k_2}\mathcal{D}_{k_2}(d_{k_1}^{(q,p)}P_{k_1 k_2}^{(q-p)} + d_{k_1 k_2}^{(q,p)}P_{k_1}^{(q-p)})$$
$$- 2\mathcal{D}_{k_1 k_2}\mathcal{D}_{k_1}(d_{k_2}^{(q,p)}P_{k_1 k_2}^{(q-p)} + d_{k_1 k_2}^{(q,p)}P_{k_2}^{(q-p)})], \tag{73}$$

$$Y_5(q,p;k_1,k_2) = \overline{\Delta}^{-2}(d_{k_1}^{(q,p)}P_{k_2}^{(q-p)} + d_{k_2}^{(q,p)}P_{k_1}^{(q-p)}$$
$$- 2d_{k_1 k_2}^{(q,p)}P_{k_1 k_2}^{(q-p)}), \tag{74}$$

$$Y_6(q;k_1,k_2) = \mathcal{D}_{k_1}d_{k_1}^{(q)}P_{k_2,k_2} + \mathcal{D}_{k_2}d_{k_2}^{(q)}P_{k_1,k_1}$$
$$+ 4\mathcal{D}_{k_1 k_2}d_{k_1 k_2}^{(q)}P_{k_1 k_2,k_1 k_2}$$
$$+ (\mathcal{D}_{k_1}d_{k_2}^{(q)} + \mathcal{D}_{k_2}d_{k_1}^{(q)})P_{k_1,k_2}$$
$$- 2(\mathcal{D}_{k_2}d_{k_1 k_2}^{(q)} + \mathcal{D}_{k_1 k_2}d_{k_2}^{(q)})P_{k_1,k_1 k_2}$$
$$- 2(\mathcal{D}_{k_1}d_{k_1 k_2}^{(q)} + \mathcal{D}_{k_1 k_2}d_{k_1}^{(q)})P_{k_2,k_1 k_2}. \tag{75}$$

We have also denoted

$$P_k^{(s)} = \sum_p d_k^{(p,p+s)}\varphi_{p,p+s}, \tag{76}$$

$$P_{k_1,k_2} = \overline{\Delta}^{-2}\sum_s P_{k_1}^{(s)}P_{k_2}^{(s)} = \overline{D_{k_1}D_{k_2}}^{(c)}. \tag{77}$$

Here each index, e.g., k_1, can actually be a pair $k_1'k_2'$, in which case $d_{k_1'k_2'}^{(q,p)}$ is assumed to be used instead of $d_{k_1}^{(q,p)}$. The latter is a linear combination of the former [see Eq. (25)].

Finally, we would like to rewrite the mean energy in these notations

$$\frac{\overline{\langle H \rangle}}{N} = \frac{3\kappa}{2}\mathcal{D}_{01} + \hat{u}_2 \sum_k \frac{1}{\mathcal{D}_k^{3/2}} + \hat{u}_3 \sum_{k_1,k_2} \frac{1}{Y_0(k_1,k_2)^{3/2}}$$
$$- \frac{3}{2}\hat{1}\sum_k \frac{\Phi_k}{\mathcal{D}_k^{5/2}} + \hat{u}_2 \frac{15}{8}\sum_k \frac{P_{k,k}}{\mathcal{D}_k^{7/2}}$$
$$+ \hat{u}_3 \frac{15}{8}\sum_{k_1,k_2} \frac{Y_2(k_1,k_2)}{Y_0(k_1,k_2)^{7/2}} - \hat{u}_3 \frac{3}{2}\sum_{k_1,k_2} \frac{Y_3(k_1,k_2)}{Y_0(k_1,k_2)^{5/2}}. \tag{78}$$

C. Equilibrium distributions

Here we shall show that at equilibrium and to order $\overline{\Delta}^2$ our nonequilibrium method generates the same set of equations as the variational Gibbs-Bogoliubov approach for equilibrium. This is not obvious because we perform averaging over the quenched disorder. This derivation will also help to explain why the use of the replica trick may be avoided in our method.

Now, given the trial Hamiltonian (37), the free energy estimate will be

$$\mathcal{A} = \mathcal{A}_0 + \overline{\langle (H-H_0)\rangle_0}, \quad \mathcal{A}_0 = \frac{3\beta^{-1}}{2}\overline{\mathrm{Tr}\,\ln V(\{\lambda\})}, \tag{79}$$

where $\mathcal{A}_0$ is the free energy associated with H_0 and the matrix $V(\{\lambda\})$ is given by Eqs. (11) and (41). If one can perform the disorder averages directly, as we do by applying the perturbation theory in $\overline{\Delta}^2$, there is no need to introduce n copies of the system and take the limit $n\to 0$. First, we calculate the main observables

$$\mathcal{F}_q = \beta^{-1} \overline{[V(\{\lambda\})^{-1}]}_{qq} = \frac{\beta^{-1}}{V_q} \left(1 + \overline{\Delta}^2 \sum_p \frac{U_{qp}^2}{V_q V_p} \right) + O(\overline{\Delta}^4),$$
(80)

$$\varphi_{qp} = \beta^{-1} \overline{[V(\{\lambda\})^{-1}]}_{qp} \lambda_{q-p} = -\beta^{-1} \overline{\Delta}^2 \frac{U_{qp}}{V_q V_p} + O(\overline{\Delta}^4).$$
(81)

Now let us set the time derivatives to zero in the equations of motion (43) and (44). Resolving those equations up to order $\overline{\Delta}^2$, one immediately recovers Eqs. (80) and (81). In a similar manner we obtain for the entropic contribution

$$\mathcal{S} = -k_B \frac{3}{2} \overline{\mathrm{Tr} \ln V(\{\lambda\})}$$

$$= -k_B \frac{3}{2} \sum_q \ln V_q + k_B \frac{3\overline{\Delta}^2}{4} \sum_{q,p} \frac{U_{qp}^2}{V_q V_p} + O(\overline{\Delta}^4). \quad (82)$$

Calculation of the mean energy $\mathcal{E} = \overline{\langle H \rangle}$ gives the same result as that of Sec. III B [see Eq. (78), where it is assumed that $\mathcal{F}_q$ and φ_{qp} are expressed via the effective potentials V_q and U_{qp} by Eqs. (80) and (81)]. Minimization of the free energy $\mathcal{A}[V_q, U_{qp}] = \mathcal{E} - TS$ with respect to these variational parameters yields the self-consistent equations

$$\mathcal{F}_q = -\frac{2}{3} \frac{\partial \mathcal{E}}{\partial V_q}, \quad \varphi_{qp} = -\frac{2}{3} \frac{\partial \mathcal{E}}{\partial U_{qp}}.$$
(83)

These equations, however, seem to be different from the ones we have obtained in Sec. III B. To bring them into an equivalent form let us invert Eqs. (80) and (81),

$$V_q = \frac{\beta^{-1}}{\mathcal{F}_q} \left(1 + \overline{\Delta}^{-2} \sum_p \frac{\varphi_{qp}^2}{\mathcal{F}_q \mathcal{F}_p} \right) + O(\overline{\Delta}^4),$$
(84)

$$U_{qp} = -\beta^{-1} \overline{\Delta}^{-2} \frac{\varphi_{qp}}{\mathcal{F}_q \mathcal{F}_p} + O(\overline{\Delta}^2),$$
(85)

where we have discarded the $\overline{\Delta}^2$-order term in U_{qp} since it always appears in the equations multiplied by $\overline{\Delta}^2$. This allows us to reexpress the entropy

$$\mathcal{S} = k_B \frac{3}{2} \sum_q \ln \mathcal{F}_q - k_B \frac{3\overline{\Delta}^{-2}}{4} \sum_{q,p} \frac{\varphi_{qp}^2}{\mathcal{F}_q \mathcal{F}_p} + O(\overline{\Delta}^4). \quad (86)$$

Minimization of the free energy $\mathcal{A}[\mathcal{F}_q, \varphi_{qp}]$ over its variational parameters now gives the self-consistent equations

$$V_q = \frac{2}{3} \frac{\partial \mathcal{E}}{\partial \mathcal{F}_q}, \quad U_{qp} = \frac{2}{3} \frac{\partial \mathcal{E}}{\partial \varphi_{qp}},$$
(87)

which do indeed coincide with the formulas for these effective potentials obtained from kinetics (67) and (68). Thus we have proved that at the first order of the perturbation expansion the fixed point of our kinetic equations precisely agrees with the extremal point of the free energy obtained in the Gibbs-Bogoliubov method.

Finally, the kinetic equations themselves (43) and (44) now may be rewritten in terms of the derivatives of the free energy $\mathcal{A}$ with respect to the dynamical variables as

$$\frac{\zeta}{2} \frac{d}{dt} \mathcal{F}_q(t) = -\frac{2}{3} \left(\mathcal{F}_q \frac{\partial \mathcal{A}}{\partial \mathcal{F}_q} + \sum_p \varphi_{qp} \frac{\partial \mathcal{A}}{\partial \varphi_{qp}} \right), \quad (88)$$

$$\zeta \frac{d}{dt} \varphi_{qp}(t) = -\frac{2}{3} \left(\varphi_{qp} \left(\frac{\partial \mathcal{A}}{\partial \mathcal{F}_q} + \frac{\partial \mathcal{A}}{\partial \mathcal{F}_p} \right) + \overline{\Delta}^2 (\mathcal{F}_q + \mathcal{F}_p) \frac{\partial \mathcal{A}}{\partial \varphi_{qp}} \right).$$
(89)

This form of the kinetic equations has a transparent meaning. Indeed, the folding kinetics could be understood as a motion on the surface of the free energy parametrized by dynamical variables $\mathcal{F}_q, \varphi_{qp}$. The motion is determined by gradients and is directed towards the global energy minimum. Here the free-energy landscape determining the kinetics represents the flow of the whole statistical ensemble. individual

IV. NUMERICAL RESULTS

In this section we present our results from numerical solution of the self-consistency equations (43) and (44). We shall be interested in the kinetics of folding caused by an abrupt quench from the extended Flory coil (positive $\overline{u}_2$, $\Delta = 0$) to the region of the phase diagram corresponding to negative second virial coefficient $\overline{u}_2$ and nonzero dispersion of disorder Δ. Then, after the quench, the self-consistent equations are solved using the modified Runge-Kutta scheme [38] analogous to that of Refs. [36,35]. We account for the excluded-volume effect only up to the three-body interaction. Inclusion of the four-body interaction is required for sufficiently large Δ, but it is unnecessary for the dispersions considered in this paper.

Our present analysis is still far from exhaustive. A complete numerical study of the problem would require a separate and rather lengthy work. Thus our purpose here is just to make an initial reconnaissance into the variety of complex phenomena embodied in the set of equations (43) and (44) together with Eqs. (67) and (68). Our understanding of their solution in analytical terms is still rather limited apart from a few simple limiting regimes. Implementation of the code for numerical integration of these equation in itself presented a technical challenge in comparison to a relatively trivial homopolymer [36] and apparently more complicated ''ab'' block copolymer [35]. It is worthwhile mentioning also that the computational time required for the solution of this problem is about N times longer than for those simpler problems mentioned above. Even this has been achieved by extensive accounting of all possible symmetries and summation reduction techniques. Thus we have managed to study chains of up to 50 monomers and in principle one can reach up to hundreds of units given the best computational resources available. Every effort has been made to control precision of integration and ensure stability of solution. There are other minor technicalities that are irrelevant for this theoretical paper and we hope to address them elsewhere.

It is natural to work with the combinations $\mathcal{L} = (k_B T/\kappa)^{1/2}$ and $\mathcal{T} = \zeta_b/\kappa$ as the units of size and time in the system. In the following we have used the following particular choice of parameters: $k_B T = 1$, $\kappa = 1$, and $\zeta_b = 1$,
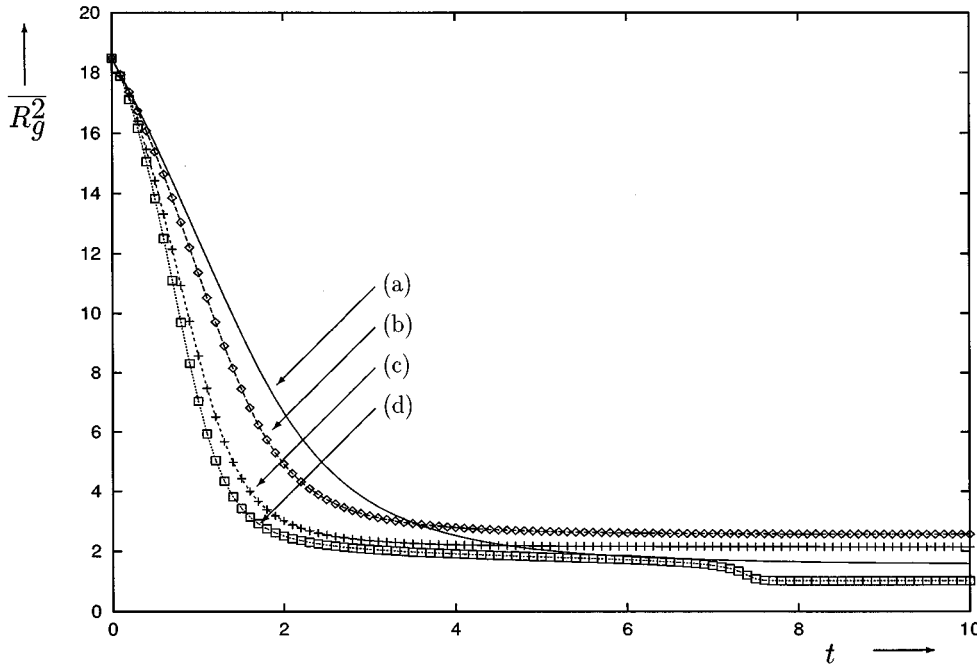
FIG. 1. Plots of the mean-squared radius of gyration $\overline{R_g^2}$ (in units $\mathcal{L}^2$) vs time t (in units $\mathcal{T}$). Lines (a)–(d) correspond respectively to the values of the dispersion of disorder $\Delta = 0$ (homopolymer), 16, 32, and 40 (in units $k_B T \mathcal{L}^3$). In this figure and Figs. 2–5 the values of the parameters are the following: the degree of polymerization $N = 40$, the third virial coefficient $\overline{u}_3 = 10$ (in units $k_B T \mathcal{L}^6$), the initial and final second virial coefficients $\overline{u}_2^{(i)} = 15$ and $\overline{u}_2^{(f)} = -25$ (in units $k_B T \mathcal{L}^3$), and the initial dispersion of disorder $\Delta^{(i)} = 0$.

which fix $\mathcal{L}$ and $\mathcal{T}$ to be equal to unity.

Note that $q = 0$ corresponds to the diffusive mode. It does not affect the intramolecular conformational modes and therefore will not be considered. There are many interesting observables that may be calculated, but we shall concentrate only on a few global ones giving most important information.

In Fig. 1 we draw the time evolution of the mean-squared radius of gyration $\overline{R_g^2}$ for different dispersions of disorder Δ. The solid line (a) corresponds to a homopolymer ($\Delta = 0$) and serves as a reference line for recognizing the effect of randomness. The first kinetic stage appears to be universal in accord with our theoretical expectations [35] and the chain is an effective homopolymer. Here the effect of randomness is negligible and all curves nearly coincide. During this stage the spinodal decomposition in the internal metric of the chain [39] leads to a necklace of small locally collapsed clusters [29,28,36], and for not too deep quenches the radius of gyration falls according to the power law $\overline{R_g^2}(t) = \overline{R_g^2}(0) - A t^{7/11}$. Although the overall spinodal picture of the first stage is correct, the local structure of the clusters that are forming is different from those in the homopolymer.

The deviation between different Δ curves signifies the onset of the second or ''coarsening'' kinetic stage. There the random copolymer behaves very much like the periodic heteropolymer of Ref. [35] as the memory effects are still rather small. We see that the collapse proceeds faster than that of the homopolymer because now the rate of collapse is predominantly determined by hydrophobic units [35]. Further behavior depends on the value of the dispersion. For weak disorder [curves (b) and (c)] $\overline{R_g^2}(t)$ reaches eventually its final value, which is greater than for the homopolymer, again in agreement with the periodic ab heteropolymer. However, for a dispersion larger than some critical value, denoted by Δ_r [curve (d)], we observe that after a long plateau, where $\overline{R_g^2}(t)$ decreases very slowly, at some moment τ it undergoes

a rapid final shrinking towards the state more compact than the homopolymeric globule. This picture has an interesting resemblance to the protein folding kinetics observed experimentally. However, to feel more confident with such an analogy, let us proceed and consider other observables.

In Fig. 2 we exhibit the time dependence of the phase separation order parameter Ψ, defined by Eq. (62) for different dispersions of disorder. This quantity is identically zero for a homopolymer and remains small for very weak disorder. For early times $\Psi(t)$ rapidly grows reaching its maximum near the end of the spinodal stage. This reflects the formation of the microphase structure of growing clusters, which tend to have a hydrophilic exterior and hydrophobic core [40]. During most of the coarsening stage Ψ changes only slightly. Indeed, the microdomain structure of the coalescing globule has already been formed. It is represented by the original clusters, which essentially preserve their integrity within the macroglobule. If Δ is insufficiently large, the folding ends up after optimization of the relative positions of these subclusters and the surface area. However, for stronger disorder $\Delta > \Delta_r$ (two upper curves), at some moment around τ the system undergoes further and abrupt phase separation on larger scales. This phenomenon has an obvious similarity to that of the phase separation order parameter Z in periodic heteropolymers (see Fig. 4 of Ref. [35]).

Now let us compare these observations with the behavior of the glass order parameter $\overline{R_g^2 R_g^{2(c)}}$ presented in Fig. 3. The latter can behave in a rather diverse manner depending on the value of Δ. We can distinguish at least four different regimes listed in order of increasing Δ and designated by the curves labeled below as in the figure: the quantity (a) is almost zero during the first stage and then grows during the second, but after reaching the maximum falls down to zero; (b) is very similar to case (a), but after the maximum and certain decrease, it starts to grow once again and finally tends to a nonzero value; the regime of (c) and (d) is similar to (a) and
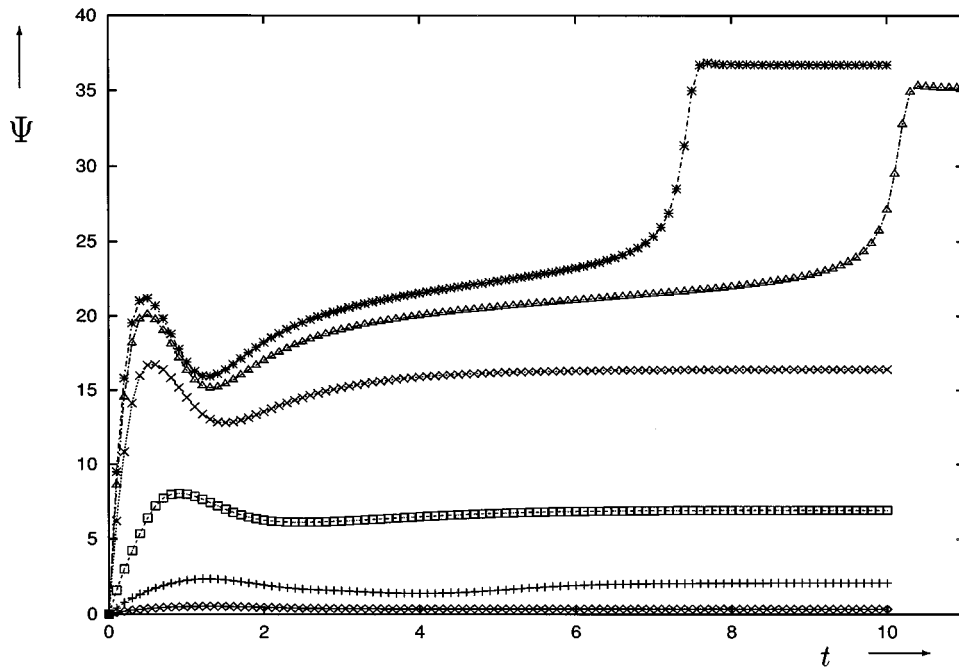
FIG. 2. Plots of the phase separation order parameter Ψ (in units $k_B T \mathcal{L}^5$) vs time t (in units $\mathcal{T}$) for different values of the dispersion of disorder (from bottom to top): $\Delta = 4, 8, 16, 32, 38,$ and 40 (in units $k_B T \mathcal{L}^3$).

(b) first, but after reaching its maximum decreases slightly and remains at a high level, where it finally remains; the regime of (e) and (f) is the same as above, but after the critical dispersion Δ_r it falls rapidly to a level very close to zero. Comparing this with Fig. 2, we find that the critical dispersion is, in fact, the same for glassy and phase separation order parameters.

Thus to resume, other the system is strongly frustrated during the coarsening stage and forms a sort of glass. The frustration is induced by the hydrophilic shells of the sub-

clusters and by the polymeric bonds. Thus the system is kinetically arrested and possesses, as we shall see below, a long relaxation time due to the height of potential barrier. The existence of such a glassy structure is clearly manifested in the glass order parameter $\overline{R_g^2 R_g^{2}}^{(c)}$. Thus Fig. 3 tells us that there are at least three different final phases of the system distinguished by the glass order parameter: for small Δ there is a liquidlike globule (LG), which is akin to an ordinary homopolymer globule with zero glass order parameter, and a glassy phase (G) with nonzero $\overline{R_g^2 R_g^{2}}^{(c)}$; for $\Delta > \Delta_r$ there is a
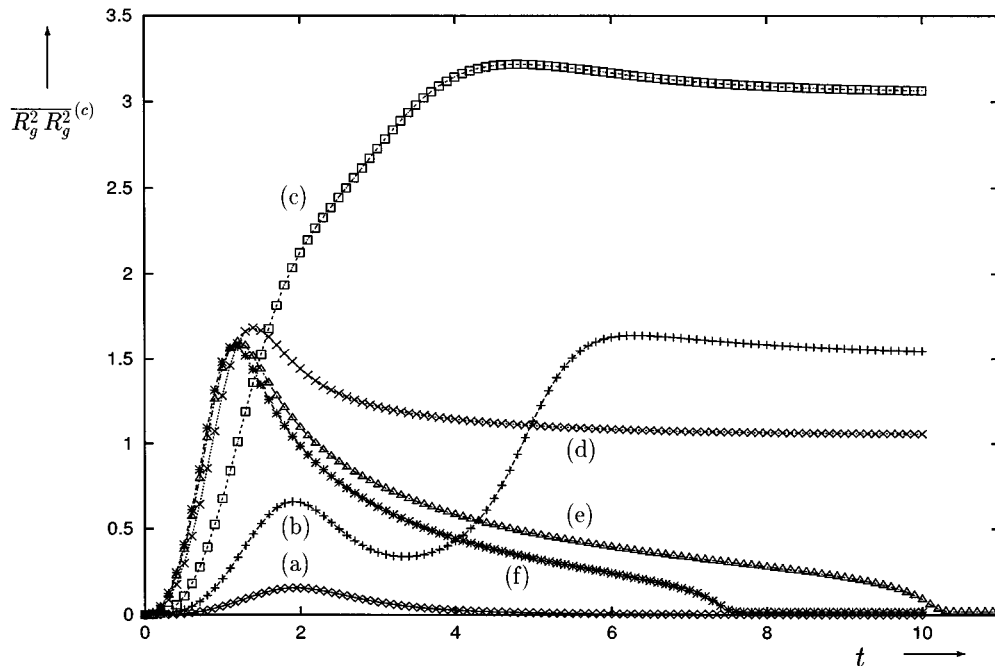
FIG. 3. Plots of the sample to sample fluctuation of the squared radius of gyration $\overline{R_g^2 R_g^{2}}^{(c)}$ (in units $\mathcal{L}^4$) vs time t (in units $\mathcal{T}$). Lines (a)–(f) correspond respectively to the values of the dispersion of disorder $\Delta = 4, 8, 16, 32, 38, 40$ (in units $k_B T \mathcal{L}^3$).
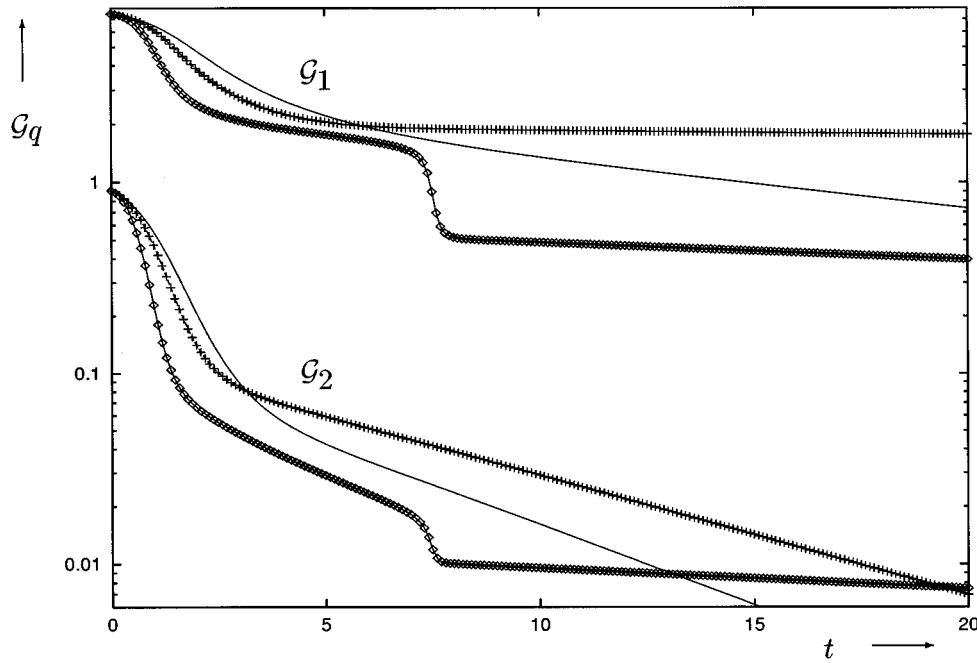
FIG. 4. Plots of the autocorrelation functions $\mathcal{G}_q(t,0)$ (in units $\mathcal{L}^2$) for $q=1,2$ vs time t (in units T) during kinetics after the quench for different values of the dispersion of disorder: $\Delta=0$ (solid lines), $\Delta=16$ (crosses), and $\Delta=40$ (diamonds).

folded phase (F) characterized by (almost) vanishing glass order parameter and a large-phase-separation order parameter. As is already becoming clear and will be shown more convincingly below, the glassiness is destroyed by the final larger-scale phase separation. The globule acquires a more organized internal structure and becomes more compact. These observations are quite striking. globule, and In broad terms the states predicted here are very close to those that have been discussed for real proteins [2].

Now, then, it would be of great interest to check the autocorrelation function (45) for further evidence in favor of glassy behaviour. The function $\mathcal{G}_1(t,0)$ is drawn in Fig. 4. The homopolymer (solid line) possesses only two characteristic relaxations: $\mathcal{G}_1(t,0) \sim e^{-\Omega_1 t}$ for very early times (the Einstein regime) and then another exponential relaxation regime $\mathcal{G}_1(t,0) \sim e^{-(V_1/\zeta)t}$ for late times [27]. The relaxation towards the F phase (diamonds) first also has the Einstein regime for very short times and then it could be described by the fast β relaxation $\mathcal{G}_1(t,0) \sim Q+C_\beta t^{-\beta}$, $t \lesssim \tau_\beta$, and then by a slow α relaxation $\mathcal{G}_1(t,0) \sim Q-C_\alpha t^\alpha$, $t \lesssim \tau_\alpha$, which finally turns into an exponential (or perhaps stretched exponential) decay. As the dispersion of disorder becomes smaller and we approach the glassy G phase (crosses in Fig. 4), the characteristic scale of α relaxation becomes very long.

The delay time near the transition line may be estimated with good precision as a power law $\tau \simeq A(\Delta-\Delta_r)^{-\gamma}$ and the parameters A, Δ_r, and γ from the fitting are presented in Table I. For quenches to the folded state but close to the renaturation transition line the delay time diverges as a power law with the exponent approximately equal to $\gamma=1/2\pm0.04$. This delay time τ also grows with the degree of polymerization N since the prefactor scales as $A \sim N^{5/3\pm0.12}$. The critical dispersion of this transition Δ_r increases significantly with N as well, but to determine the concrete form of this law one would need data for bigger systems. Thus, in the G phase there is a very pronounced

plateau in the autocorrelation function, as well as in the mean energy in Fig. 5. These laws are reminiscent of other spin-glass systems [41,42] and hence justify our interpretation of the glassy phase. If the system has been quenched to the G phase, the autocorrelation function does not decay to zero for a macroscopically long times, but remains at some constant analogous to the Edwards-Anderson order parameter in the spin-glass theory.

Having discussed the kinetics of folding, let us turn our attention to the final state of kinetics, i.e., the equilibrium phase structure of the model. We should note that the final state of kinetics may only correspond to one of all possible fixed points of the self-consistent equations. A more general analysis of the equilibrium phase diagram would be of interest. However, what we shall examine below is important primarily because it matches the notion of renaturation as a kinetic phenomenon. In Fig. 6 we draw the final value of the glassy order parameter $\overline{R_g^2 R_g^{2(c)}}$ vs the dispersion of disorder Δ for different values of the third virial coefficient. There we indeed observe the two phase transitions discovered above. When the dispersion of disorder reaches the critical value Δ_f, which scales as a positive power of u_3, the system un-

TABLE I. Values of the parameters A, Δ_r, and γ in the delay time $\tau=A(\Delta-\Delta_r)^{-\gamma}$ for polymers with different degrees of polymerization N. These parameters have been obtained from the analysis of the kinetics for different quench depths with $\Delta \gtrsim \Delta_r$. Values of the second and third virial coefficient are $\overline{u}_2=-25$ and $\overline{u}_3=10$. From these data one can obtain the scaling law $A \sim N^{1.67\pm0.12}$.

N	A	Δ_r	γ
20	5.3	17.82	0.54
30	9.1	25.96	0.50
40	16.7	35.44	0.54
50	23.6	77.43	0.47
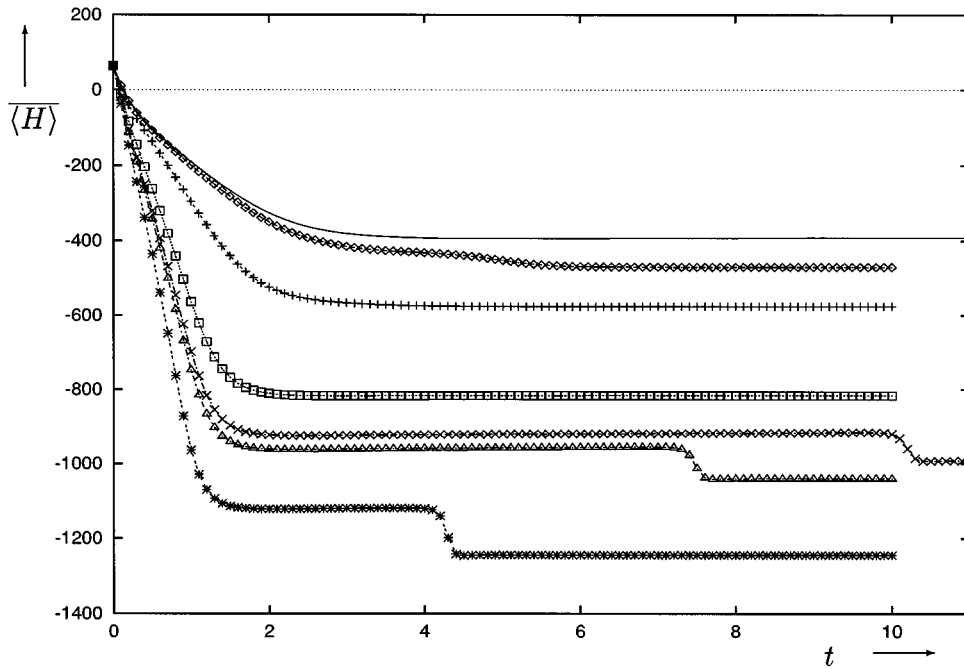
FIG. 5. Plots of the mean energy $\overline{\langle H \rangle}$ (in units $k_B T$) vs time t (in units $\mathcal{T}$) for different values of the dispersion of disorder (from top to bottom): $\Delta = 0$ (homopolymer), 8, 16, 32, 38, 40, and 48 (in units $k_B T \mathcal{L}^3$).

dergoes the *freezing* transition accompanied by an abrupt increase of the glass order parameter. Our data are in qualitative agreement with the earlier result [43] that $\Delta_f \sim \sqrt{s}/\rho$, where s is the chain flexibility and ρ is the globule density. At this phase transition the phase-separation order parameter presented in Fig. 7 changes quite regularly. In fact, Ψ grows linearly until the second *renaturation* transition, at Δ_r, where it has a rapid jump and then further grows linearly. Remarkably, the glass order parameter quickly drops to almost zero at the point Δ_r. In Table II we present the values of Δ_r for different second virial coefficients $|\bar{u}_2|$. Note that the critical dispersion changes only slightly as u_3 grows.

The reason why we may conjecture this transition to be

related to the renaturation becomes clear from Fig. 8. The homopolymer correlations of monomer positions [curve (a)] $\mathcal{D}_k$ satisfy the scaling law $\mathcal{D}_k \sim k$ for $|k| < N^{2/3}$ and $\mathcal{D}_k \sim N^{2/3}$ otherwise [36,44]. This law is preserved as one switches on the dispersion of disorder, and it is still fulfilled in the glassy phase [curves $(b)-(d)$]. The renaturation transition, however, leads to a striking modification of this law: $\mathcal{D}_k \sim$ const for any but very small k [see curve (e)].

Thus the correlations of monomer coordinates do not depend on their chain indices after we have integrated over all possible complexions of disorder. They are equal to a universal constant entirely determined by the excluded-volume interaction structure. Let us leave this idealized random co-
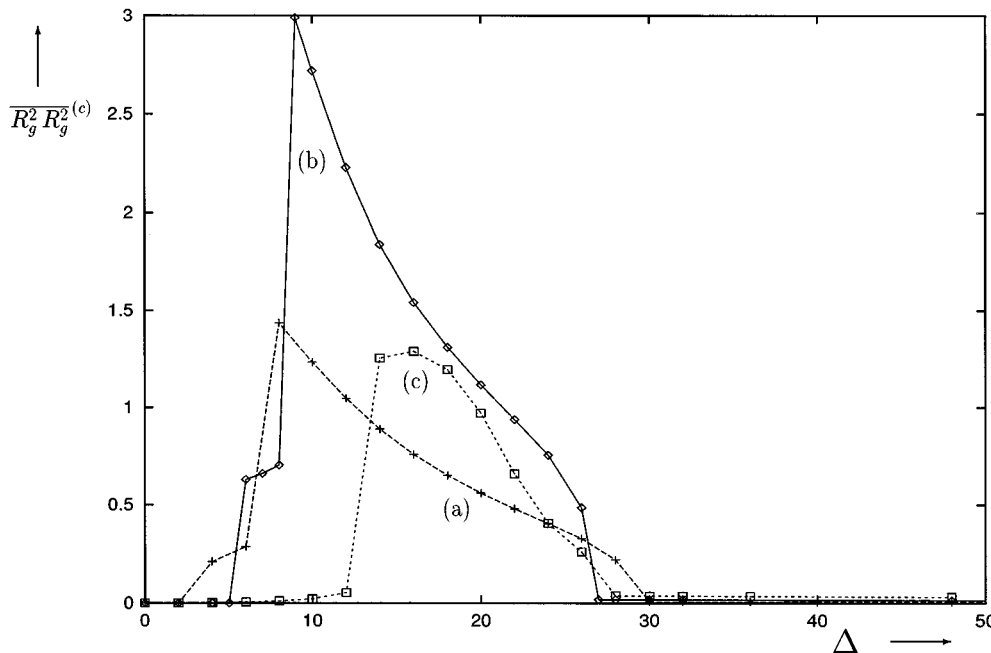
FIG. 6. Plots of the sample to sample fluctuation of the squared radius of gyration $\overline{R_g^2 R_g^{2}}^{(c)}$ (in units $\mathcal{L}^4$) vs the dispersion of disorder Δ (in units $k_B T \mathcal{L}^3$). Lines $(a)-(c)$ correspond respectively to the values of the third virial coefficient $\bar{u}_3 = 5$, 10, and 20 (in units $k_B T \mathcal{L}^6$). The degree of polymerization and the second virial coefficient are $N = 30$ and $\bar{u}_2 = -25$ (in units $k_B T \mathcal{L}^3$).
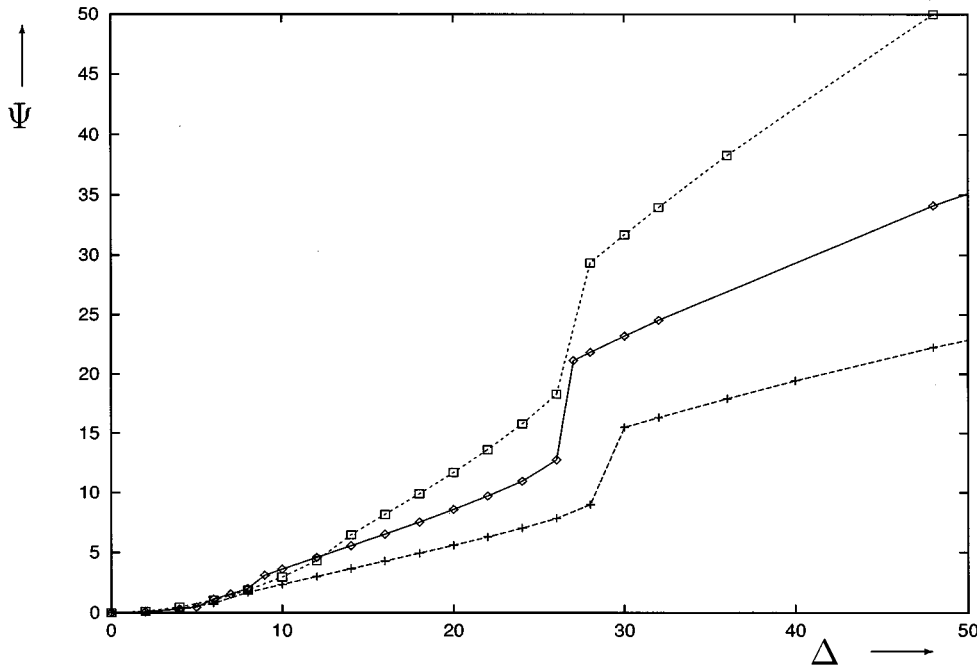
FIG. 7. Plots of the phase-separation order parameter Ψ (in units $k_B T \mathcal{L}^5$) vs the dispersion of disorder Δ (in units $k_B T \mathcal{L}^3$) for different values of the third virial coefficient (from bottom to top): $\bar{u}_3 = 5$, 10, and 20 (in units $k_B T \mathcal{L}^6$). The degree of polymerization and the second virial coefficient are $N = 30$ and $\bar{u}_2 = -25$ (in units $k_B T \mathcal{L}^3$).

polymer for a moment and consider a real protein in the native state. There one should have a unique structure of $D_{mm'}$ encoded in the primary structure, i.e., the sequence of Λ_m. As we lose the information about a particular sequence by averaging over the quenched disorder, clearly, $\mathcal{D}_{mm'}$ can only become a constant. This phenomenon, so conspicuous in our approach, is intuitively natural for real proteins in the *native* state.

Finally, let us discuss the mean-squared radius of gyration $\overline{R_g^2}$ vs the dispersion Δ drawn in Fig. 9. Generally speaking, the size of the polymer is almost independent of Δ in the LG phase, becomes larger in the glassy phase, and is much smaller in the F phase. Thus the globule in the native state is more compact than the homopolymer one and depends weakly on the dispersion of disorder. These properties conform to the intuitive idea that a glassy globule should be bigger since parts of the chain are frozen in not completely compacted locations and that the native globule should be maximally compacted due to the best possible optimization of the volume interactions. Moreover, the mean energy (see

Fig. 5) becomes smaller in the native state as well. This may be interpreted by arguing [3] that the system occupies the ground state separated by a gap from higher-energy levels, while it is trapped in some higher, but relatively low-energy, level in the glassy phase.

V. CONCLUSION

In this work we have developed an approach for studying kinetics of random copolymer conformational changes and discussed the potential relations to the protein folding problem. Our method presents an extension of the Gaussian self-consistent approach, which has been successfully applied by us to a homopolymer and periodic heteropolymers. It may be actually viewed as a version of the method for arbitrary heteropolymers with a disorder-dependent effective potential. The latter, however, is rather awkward in practice, particularly for numerical solution, since all averaged quantities are nondiagonal in the Fourier variables. The diagonality is recovered after the integration over the quenched disorder, but in a quite nontrivial way. Thus the two-point correlations (see the Appendix) are strictly diagonal, but any three- and four-point objects are not. However, they are expressed in a relatively simple way through the main variables $\mathcal{F}_q$ and φ_{qp}. These properties lead eventually to the reduction of one summation in the mean energy and effective potentials.

Although some of our derivations were performed only up to order Δ^2, the properties above are valid at all orders. Because we have used the fully dressed quantities $\mathcal{D}_k$ and an enforced closure of the Bogoliubov chain rather than the perturbation theory, one may expect that our equations are actually valid for moderate dispersions (see [37]).

The richness of the dynamical variables (or variational parameters for equilibrium) allows us to achieve certain success in this complicated problem. Even a preliminary numerical analysis has led to a number of interesting insights. For example, we have obtained a qualitatively correct picture

TABLE II. Values of the critical dispersion Δ_r for the folding transition vs the second virial coeficient $\bar{u}_2$ for polymer with the degree of polymerization $N = 30$. The value of the third virial coefficient is $\bar{u}_3 = 10$.

u_2	Δ_r
−15	14.0
−17	14.1
−20	17.0
−25	25.96
−30	32.3
−35	38.7
−40	45.2
−50	59.3
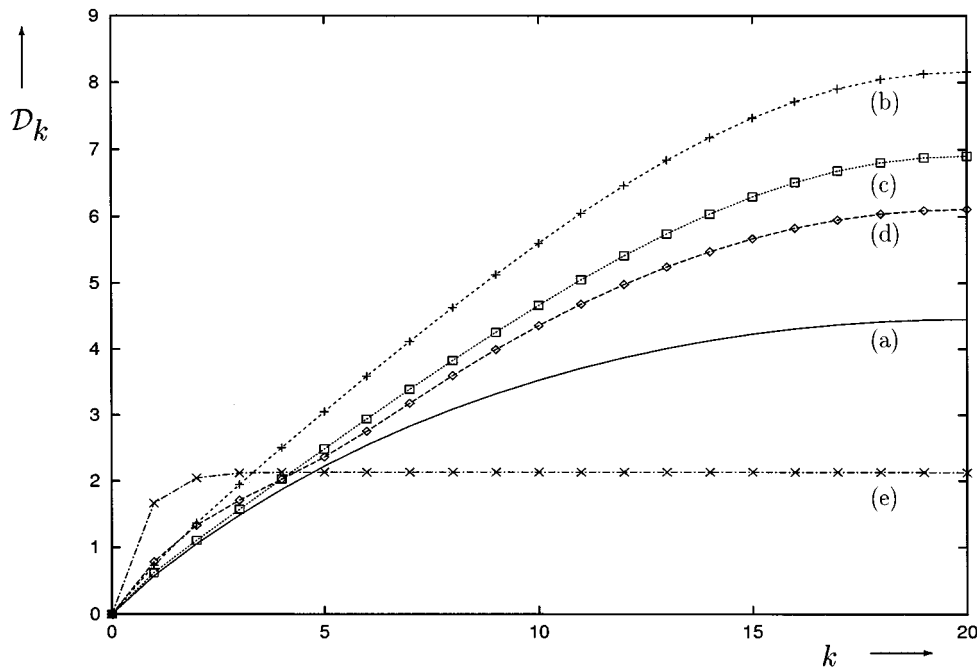
FIG. 8. Plots of the equilibrium correlations of monomer coordinates [45] $\mathcal{D}_k$ (in units $\mathcal{L}^2$) vs the chain index k for polymer with the degree of polymerization $N = 40$ and values of the second and the third virial coefficients $\bar{u}_2 = -25$ (in units $k_B T \mathcal{L}^3$) and $\bar{u}_3 = 10$ (in units $k_B T \mathcal{L}^6$). Lines $(a)-(e)$ correspond respectively to the values of the dispersion of disorder $\Delta = 0$ (homopolymer), 16, 32, 8, and 38 (in units $k_B T \mathcal{L}^3$).

for kinetics of protein folding. This kinetics yields spin-glass-like relaxations for the autocorrelation function. Investigation of the final state of kinetics has given the phase structure of the system with three globular phases: liquid globulelike, glassy, and folded. The glassy phase probably corresponds to the molten globule, while the folded one has many features suggesting its relation to the native state of proteins. The most important discovery here is the law $\mathcal{D}_k \simeq$ const for the spatial correlations of monomer coordinates. We have observed what we believe to be correct behavior for such observables as the mean-squared radius of gyration, the mean energy, and the phase-separation order

parameter in all three phases. Renaturation, or the transition to the native state, has been explained as the large-scale phase separation that destroys the glassy structure.

We have also proposed a simple explanation of the kinetics of folding based upon the *necklace* mechanism of the early stages. Freezing occurs due to strong frustration after coalescence of locally phase-separated clusters. On the contrary, renaturation is the process of global energy optimization proceeding by larger-scale phase separation that destroys the glassiness.

It is encouraging that our conclusion about the existence of the three different collapsed states, liquid globule, frozen,
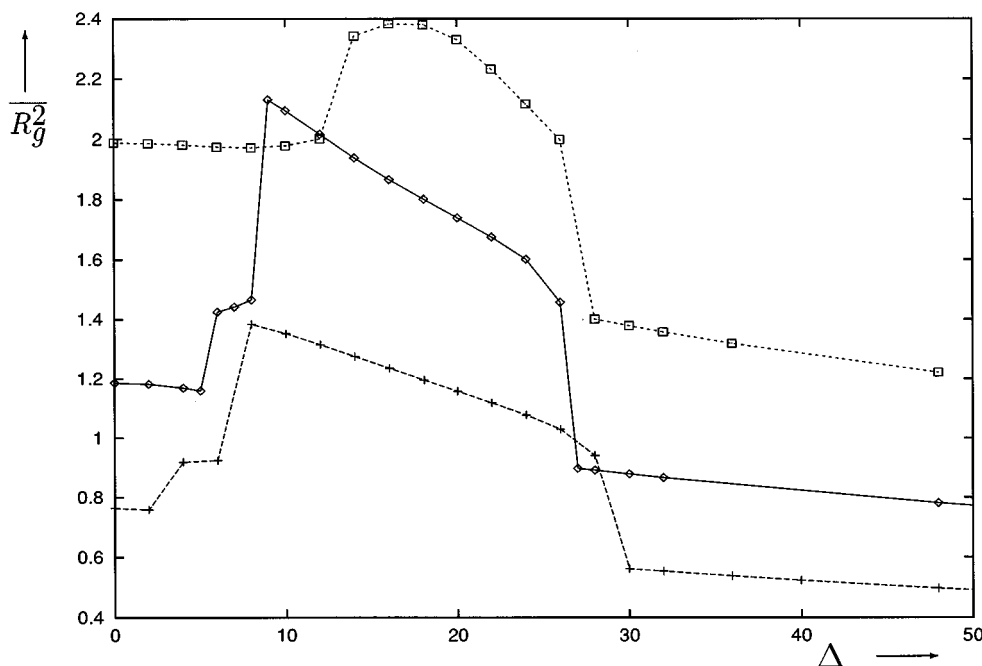
FIG. 9. Plots of the equilibrium mean squared radius of gyration $\overline{R_g^2}$ (in units $\mathcal{L}^2$) vs the dispersion of disorder Δ (in units $k_B T \mathcal{L}^3$) for different values of the third virial coefficient (from bottom to top): $\bar{u}_3 = 5$, 10, and 20 (in units $k_B T \mathcal{L}^6$). The degree of polymerization and the second virial coefficient are $N = 30$ and $\bar{u}_2 = -25$ (in units $k_B T \mathcal{L}^3$).

and folded, agrees with that of the Monte Carlo simulations on a lattice [25] and that in other simulations [10] the kinetics proceeds in several stages with an activated final folding. The Gaussian distribution of random sequences is perhaps sufficiently wide to include many good folding sequences studied in Monte Carlo and their contribution is substantial enough to exhibit something like the folded state after disorder averaging. Clearly, the averaging over disorder is necessary if we are to extract universal, or at least generic, laws. On the other hand, the Gaussian distribution is really too large and future works must be directed at averaging over more refined distribution, appropriate for the protein folding problem.

Nevertheless, we believe that the results shown here present an important advance in understanding qualitative aspects of the kinetics of protein folding using the methods of nonequilibrium statistical mechanics. We accept that much remains to be accomplished. First, the scalings of the various order parameters and universal exponents must be extracted, a nontrivial task requiring extensive numerical study and analytical insight. Second, efforts must be made to establish connection to experiment in these systems and existing protein data bases, whatever relevant information is available for typical globular proteins with only between 200 and 500 amino acid residues.

In completing the purely theoretical aspects of this program there now appear to be only technical obstacles remaining. Whether the information yielded thereby will affect substantially the detailed understanding of the folding process of real proteins is a question that must await later judgements.

ACKNOWLEDGMENTS

APPENDIX A: PROOF OF THE DIAGONALITY OF $\overline{\langle \mathbf{x}_{q'} \mathbf{x}_q \rangle}$

The formal integration of the linear ensemble (10) gives

$$\mathbf{x}_q(t) = \frac{1}{\zeta} \int_0^t dt' (-V_q \mathbf{x}_q - W_{qp} \mathbf{x}_p + \boldsymbol{\eta}_q)(t'), \quad \text{(A1)}$$

where $W_{qp} \equiv \Sigma_r U_{q,p,r} \Lambda_r$. We remark that, to generate a well-defined time evolution, the matrix W_{qp} should be real and symmetric. These properties impose two restrictions upon the coefficient functions

$$U_{-q,p,r} = U_{q,-p,-r}, \quad U_{q,p,r} = U_{p,q,-r}. \quad \text{(A2)}$$

Multiplying Eq. (A1) by itself with a different index and taking the averages, one can show that the diagonality property (34) extended for the nonequal-time correlations $\overline{\langle \mathbf{x}_{q'}(t') \mathbf{x}_q(t'') \rangle} \sim \delta_{-q,q'}$ implies the orthogonality relation

$$\sum_r U_{q,p,r}(t') U_{q',-p,-r}(t'') = \delta_{-q,q'} \mathcal{C}_{qp}(t',t''), \quad \text{(A3)}$$

with $\mathcal{C}_{qp}$ being some functions. This constraint is really quite restrictive since the index r in $U_{q,p,r}$ turns out to be linearly dependent on the indices q,p. By a direct check it is now trivial to see that the special form (41) indeed satisfies relations (A2) and (A3).

[1] *Protein Folding*, edited by T. E. Creighton (Wiley, New York, 1992); *New Developments in Theoretical Studies of Proteins*, edited by R. Elber (World Scientific, Singapore, 1994).

[2] H. A. Scheraga, Pure Appl. Chem. **36**, 1 (1973); N. Go and H. Taketomi, Proc. Natl. Acad. Sci. U.S.A. **75**, 559 (1978); O. Ptitsyn and A. Finkelstein, Q. Rev. Biophys. **13**, 339 (1980); P. Privalov, Adv. Protein Chem. **35**, 1 (1982); O. Ptitsyn, J. Protein Chem. **6**, 273 (1987); K. A. Dill, Biochemistry **24**, 1501 (1985); **29**, 7133 (1990); H. Frauenfelder, in *Structure and Dynamics of Nucleic Acids, Proteins and Membranes*, edited by E. Clementi and S. Chin (Plenum, New York, 1986); H. Frauenfelder, F. Parak, and R. Young, Annu. Rev. Biophys. Biophys. Chem. **17**, 451 (1988); M. Matsumoto *et al.*, J. Polym. Sci. B **30**, 779 (1992); K. Minagawa, Y. Matsuzawa, K. Yoshikawa, A. R. Khokhlov, and M. Doi, Biopolymers **34**, 555 (1994).

[3] E. Shakhnovich and A. M. Gutin, Nature **346**, 773 (1990); A. Sali, E. Shakhnovich, and M. Karplus, *ibid.* **369**, 248 (1994).

[4] C. Tanford, *The Hydrophobic Effect* (Wiley, New York, 1980); K. A. Dill, Biochemistry **29**, 7133 (1990); S. P. Obukhov, J. Phys. A **19**, 3655 (1986).

[5] P. G. Wolynes, in *Spin Glass Ideas in Biology*, edited by D. Stein (World Scientific, Singapore, 1991).

[6] M. Mezard, G. Parisi, and M. Virasoro, *Spin Glass Theory and Beyond* (World Scientific, Singapore, 1987).

[7] M. Mezard and G. Parisi, J. Phys. (France) I **1**, 809 (1991).

[8] J. D. Bryngelson and P.G. Wolynes, Proc. Natl. Acad. Sci. U.S.A. **84**, 7524 (1987); P. G. Wolynes, J. N. Onuchic, and D. Thirumalai, Science **267**, 1619 (1995).

[9] K. F. Lau and K. A. Dill, Macromolecules **22**, 3986 (1989); H. S. Chan and K. A. Dill, *ibid.* **22**, 4559 (1989); J. Chem. Phys. **95**, 3775 (1991); **96**, 768 (1992); **99**, 2116 (1993); K. A. Dill, K. M. Fiebig, and H.S. Chan, Proc. Natl. Acad. Sci. U.S.A. **90**, 1942 (1993).

[10] C. J. Camacho and D. Thirumalai, Phys. Rev. Lett. **71**, 2505 (1993); Proc. Natl. Acad. Sci. U.S.A. **90**, 6369 (1993); **90**, 1277 (1995).

[11] J. D. Honeycutt and D. Thirumalai, Biopolymers **32**, 695 (1992); D. Thirumalai, J. Phys. (France) I **5**, 1457 (1995).

[12] E. Shakhnovich, Phys. Rev. Lett. **72** 3907 (1994).

[13] P. G. de Gennes, *Scaling Concepts in Polymer Physics*, 3rd ed. (Cornell University Press, Ithaca, 1988); M. Doi and S. F. Edwards, *The Theory of Polymer Dynamics* (Oxford Science, New York, 1989); J. des Cloizeaux and G. Jannink, *Polymers*

in Solution (Clarendon, Oxford, 1990).

[14] C. D. Sfatos, A. M. Gutin, and E. I. Shakhnovich, Phys. Rev. E **48**, 465 (1993).

[15] E. I. Shakhnovich and A. M. Gutin, J. Phys. A **22**, 1647 (1989); J. Chem. Phys. **93**, 5967 (1990).

[16] V. S. Pande, A. Yu. Grosberg, and T. Tanaka, Phys. Rev. E **51**, 3381 (1995).

[17] A. V. Dobrynin and I. Ya. Erukhimovich, Pis'ma Zh. Éksp. Teor. Fiz. **53**, 545 (1991).

[18] G. Z. Archonts and E. I. Shakhnovich, Phys. Rev. E **49**, 3109 (1994).

[19] T. Garel and H. Orland, Europhys. Lett. **6**, 307 (1988); **6**, 597 (1988); G. H. Fredrickson, S. T. Milner, and L. Leibler, Macromolecules **25**, 6341 (1992); C. D. Sfatos, A. M. Gutin, and E. I. Shakhnovich, Phys. Rev. E **51**, 4727 (1995).

[20] J. D. Bryngelson, J. Chem. Phys. **100**, 6038 (1994).

[21] K. Yue and K.A. Dill, Proc. Natl. Acad. Sci. U.S.A. **89**, 4163 (1992).

[22] E. I. Shakhnovich and A.M. Gutin, Proc. Natl. Acad. Sci. U.S.A. **90**, 7195 (1993).

[23] V. S. Pande, A. Yu. Grosberg, and T. Tanaka, J. Chem. Phys. **101**, 8246 (1994); Macromolecules **28**, 2218 (1995); J. Chem. Phys. **103**, 9482 (1995).

[24] A. Dinner, A. Sali, M. Karplus, and E. Shakhnovich, J. Chem. Phys. **101**, 1444 (1994).

[25] P. E. Leopold, M. Montal, and J. Onuchic, Proc. Natl. Acad. Sci. U.S.A., **89**, 9721 (1992); N. D. Socci and J. N. Onuchic, J. Chem. Phys. **103**, 4732 (1995).

[26] E. I. Shakhnovich and A. M. Gutin, J. Phys. A **22**, 1647 (1989); E. I. Shakhnovich and A. M. Gutin, J. Chem. Phys. **93**, 5967 (1990).

[27] E. G. Timoshenko and K. A. Dawson, Phys. Rev. E **51**, 492 (1995).

[28] E. G. Timoshenko, Yu. A. Kuznetsov, and K. A. Dawson, J. Chem. Phys. **102**, 1816 (1995).

[29] Yu. A. Kuznetsov, E. G. Timoshenko, and K. A. Dawson, J. Chem. Phys. **103**, 4807 (1995).

[30] A. Yu. Grosberg, Yu. A. Kuznetsov, E. G. Timoshenko, and K. A. Dawson (unpublished).

[31] E. G. Timoshenko, Yu. A. Kuznetsov, and K.A. Dawson (unpublished).

[32] Note that modest adaptations permit us to incorporate the hydrodynamic effect. We have illustrated the method for homopolymer kinetics in a previous work in Ref. [36].

[33] This equation fundamentally represents a phantom ''network,'' which can pass through itself. We note that this is not the same as a phantom chain, and the fact that there are effective springs connected between all pairs has the effect of restraining crossing. In any case, the method has been applied to problems with known kinetic laws, and good agreement has been found. The effect of nonphantomness has been studied in Monte Carlo simulation for a homopolymer in Ref. [30]. It is quite important in the dense globular state. For an open polymer topological restrictions may be removed via self-reptations of the chain, and it has been argued that this leads to an even longer final kinetic stage with the time scale $\tau_{\text{reptations}} \sim N^3$. However, this is a delicate question that requires a separate study for heteropolymers.

[34] Really, for a ring polymer $\{\Lambda_m\}$ are defined only on a half period and symmetrically reflected to the other half by the condition $\Lambda_{N-m} = \Lambda_m$. This expresses the inversion symmetry of Ref. [35] and allows one to establish the correct correspondence of a ring with N units to an open chain with $N/2$ units (see Ref. [36] for more detail).

[35] E. G. Timoshenko, Yu. A. Kuznetsov, and K.A. Dawson, Phys. Rev. E **53**, 3886 (1996).

[36] Yu. A. Kuznetsov, E. G. Timoshenko, and K. A. Dawson, J. Chem. Phys. **104**, 3338 (1996).

[37] From these closure relations and the equations of motion (43) and (44) one can see, using the dominant balance method of Ref. [27], that the excluded-volume interactions are actually characterized by the combinations $\hat{u}_L = \overline{u}_L/(2\pi)^{3(L-1)/2}$ and the disorder by the scaling variable $\Delta^2/N(2\pi)^3$. The latter is considerably smaller than the former for the whole range of considered parameters, justifying the use of the weak-disorder expansion.

[38] W. H. Press, S. A. Teukolsky, W. T. Vetterling, and B. P. Flannery, *Numerical Recipes in C* (Cambridge University Press, Cambridge, 1992).

[39] Here the ''spinodal waves'' appear along the chain rather than in the underlying $3d$ space. They lead to formation of quasi-periodic small clusters along the chain during the first stage of kinetics. The internal modes $\mathcal{F}_q(t)$ exhibit the characteristic growth exponents similar to the treatments of spinodal decomposition by Cahn *et al.*, but for special q's, not for special $3d$ momenta $\mathbf{k}$. That is why we call this phenomenon the spinodal decomposition in the internal metric of the chain. This is discussed in more detail in Refs. [28,36].

[40] The parameter Ψ actually reflects both the macro- and microphase separations. The distinction can be made by analyzing the behavior of the internal modes $\mathcal{F}_q$ similarly to our heteropolymer work [35]. Thus a change of Ψ accompanied by fast changes of large-q modes (small distances along the chain) corresponds to the microphase separation, while a change of Ψ together with the small-q modes describes the overall restructuring of the hydrophobic and hydrophilic units. One can have a better feeling about both processes by using the visualization of individual conformations in the Monte Carlo method [29].

[41] H. Sompolinsky and A. Zippelius, Phys. Rev. Lett. **45**, 359 (1981); Phys. Rev. B **25**, 274 (1982).

[42] W. Götze and L. Sjögren, Z. Phys. B **65**, 415 (1987); J. Phys. C **21**, 3407 (1988).

[43] A. Moskalenko and K. A. Dawson, J. Chem. Phys. **103**, 9886 (1995).

[44] A. Yu. Grosberg and A. R. Khokhlov, *Statistical Physics of Macromolecules* (AIP, New York, 1994).

[45] The quantity $\sqrt{D_1}$ describes the mean distance between two nearest neighbors along the chain. From Fig. 8 one can see that in the folded state [curve (e)] this differs only in approximately 1.3 times compared to the ideal coil, for which that distance is equal to 1 in our units by definition.